

Commingled yarns of surface nanostructured glass and polypropylene filaments for effective composite properties

Edith Mäder · Christina Rothe · Shang-Lin Gao

Received: 4 October 2006 / Accepted: 21 December 2006 / Published online: 10 July 2007
© Springer Science+Business Media, LLC 2007

Abstract Developing commingled yarn technologies and understanding the fundamental interface nanostructures of reinforcement and thermoplastic filaments are of significant current interest. Previous research on commingled yarns was mainly focused on the air-jet texturing process, while the mechanical properties of the composites are strongly influenced by the impregnation homogeneity, the polymer sizing properties and consolidation process. Here, we report a unique melt spinning equipment for E-glass fiber which is compatibly combined with a melt spinning extruder to manufacture commingled yarns. The in-situ commingling enables to combine homogeneously both glass and polypropylene filament arrays in one processing step and without fiber damage compared to commingling by air texturing. Variation of processing conditions are investigated, i.e. sizings, diameter ratios, and arrangements of sizing/finish application related to intermingling of filament arrays. A rapid processing is achieved because of good intermingling and the low flow paths. We found that the sizing enables a good strand integrity with the polypropylene yarn. The interfacial adhesion can be improved with a sizing for glass fibers consisting of aminosilane and maleic anhydride grafted polypropylene film former, which results in both improved transverse tensile strength and compression shear strength. We also found that a very small amount of single-wall carbon nanotubes (SWNTs) in the sizing provides significantly improved interfacial adhesion

strength. This is attributed to the change in fracture behavior of the nano-structured interface and morphology of the model single-fiber composites.

Introduction

The hybrid yarn fabrication technology is recently developed for rapid and cost-effective processing continuous fiber reinforced thermoplastic composites, increasingly used as light weight components for passenger and commercial vehicles, rail vehicles, agricultural machineries as well as aerospace vehicles. Because of the very short flow paths of the viscous thermoplastic melt, commingled yarns offer an ideal opportunity to achieve short cycle times and it could address a number of challenging issues of traditional composites, including short time storage, long processing cycles, and high brittleness of some thermoset matrices. The theoretical and experimental approaches are employed to utilise the high potential of light weight construction and the wide possibilities to design continuous-fiber reinforced composites with thermoplastic matrices [1–3]. A number of studies have been directed toward manufacturing of commingled yarn [1–5], properties of composites made from commingled yarn and effects of processing conditions on impregnation, consolidation behavior [6–18].

The use of the textile reinforced thermoplastic composites in high performance light weight structural parts offers advantages compared to conventional constructions, particularly, in complex lightweight applications and the function-integrating multi-material design. However, it was reported that the mechanical properties of the

E. Mäder (✉) · C. Rothe · S.-L. Gao
Department of Composites, Leibniz Institute of Polymer
Research Dresden, Hohe Strasse 6, 01069 Dresden, Saxony,
Germany
e-mail: emaeder@ifpdd.de

composites were strongly influenced by the hybrid yarn impregnation homogeneity, the unidirectional/textile sub-assemblies, the sizing on the glass fiber (GF), and the consolidation processing conditions etc. The effects of hydrothermal ageing on commingled yarn glass fibers/polypropylene (PP) composites has been investigated [19]. It has been observed that an aminosilane fiber sizing protects fiber against water resulting in a diminution of the amount of absorbed water, where the interfacial interactions act as barriers during absorption and desorption. The extension and the profile of the Young's modulus of the interface between GF and PP matrix, because of interdiffusion and different chemical interactions, has been experimentally determined using Atomic force microscopy (AFM) [20]. The previous research on commingled yarns was mainly focussed on the air-jet texturing process. The literature contains few data about glass fiber/thermoplastic composites made from online hybrid yarns by simultaneous spinning and commingling of GF and PP filaments. Extensive research efforts are required on the processing behavior, the mechanical analysis of short and long term behavior, and on the reliability models for dimensioning optimization.

Considerable efforts are undertaken nowadays of the commingled yarn composites fracture behavior. It is well known that the intralaminar and interlaminar stresses result in relatively weak interlaminar fracture toughness, often leading to interlaminar failures, such as delamination, in composites under various loading conditions. To solve these significant challenges, researchers have developed 3D braided fibers as well as through-thickness stitching and a detailed review of these studies was given by Tong et al. [21]. However, these approaches have problems, such as low in-plane strengths for the 3D braided fibers and shorter tensile fatigue life and lower compression strengths for the stitched fiber laminates. Recently, extensive different studies using carbon-nanotube reinforcements in polymer composites have reported limited improvements in the bulk mechanical properties compared with traditional fiber-reinforced composites. An effective utilization of nanotube mechanical properties in composites is a long standing problem, despite huge promise, due to issues such as dispersion, alignment, and interfacial strength [22].

Here, we demonstrate an unexplored yet big opportunity for nanotubes in composites, using unique online hybrid yarns by simultaneous sizing with single-wall carbon nanotubes (SWNTs) to optimise the fiber/matrix interface properties. The main topic of this work is the investigation of commingled yarns manufactured online in comparison with those intermingled by air texturing based on our previous work [23]. Different processing routes of online spinning of hybrid yarns are considered regarding

sizing/finish application and surface nano-structuring using this online process at high speeds. We study the influence of different sizings and processing conditions of the hybrid yarns on the mechanical composite properties. To identify the tailored fiber and composite properties, other characterization tools such as GPC and DSC are used.

Experimental procedure

Materials

The commingled yarns are made by separate spinning of E-glass fiber (GF) and polypropylene (PP) filaments with different sizings/finishes, which in turn are intermingled by air-texturing process, as described elsewhere [12]. Two kinds of PP filaments are produced from either a commercial homopolymer (Borealis HH 450B) or a maleic anhydride modified polypropylene (MFR = 36 g/10 min) which was produced from isotactic homopolymer with the average molecular weight $M_w = 16 \times 10^4$ g/mol by blending with maleic anhydride grafted PP (Exxelor P1020 with $M_w = 8.6 \times 10^4$ g/mol). As polymer matrix for the single-fiber composites to perform the pull-out tests the high molecular weight homopolymer ($M_w = 29 \times 10^4$ g/mol, Borealis HD 120M) was used also blended with maleic anhydride grafted PP (Exxelor P1020 with $M_w = 8.6 \times 10^4$ g/mol) to investigate the most difficult conditions of alignment of the SWNTs due to the high melt viscosity of the polymer matrix (MFR = 8 g/10 min).

To achieve the best interfacial interaction for enhanced composite properties, we used standard commercial finishes and our PP-compatible sizings, namely *S* and *G*, respectively. As standard commercial finish *S* Fasavin HT11 (Zschimmer & Schwarz) was applied to the polypropylene filaments. The specially developed sizing *G* consisted of Aminopropyl-triethoxysilane AMEO (Degussa) and a nanodispersed polypropylene film former grafted with maleic anhydride and having an average particle size distribution of 90–100 nm and a molecular weight of $M_w = 9.4 \times 10^4$ g/mol. The sizing formulation was prepared by slow stirring the AMEO in 50% of the distilled water and further 30 min stirring to complete hydrolysis. The film former dispersion was diluted with distilled water and added to the silane solution. We explored different routes and stages to apply the sizing/finish on the both GF and PP fibers during the intermingle process. As one special case, only the GF were applied with sizings but no finish is applied to the PP-filaments. Additionally, during the continuous spinning process, the glass fibers were in-situ sized by the above described

aqueous sizing G with additional 0.04 wt% SWNTs (Nanocyl S.A., Belgium) related to the sizing.

The online hybrid yarns are made by simultaneous spinning and commingling of GF and PP filaments with fiber volume fraction of 50%. We comprised the spatial integration of a thermoplastic melt spinning equipment into the workspace of the existing equipment for processing continuous GF filaments (Fig. 1) [24]. The optimized processing condition for a homogeneous mix of the GF and PP filament arrays has been established after comparing different technological routes including the adaption of the spinning velocity and the use of applicable nozzles for the PP spinning. The melt temperatures of GF and PP are 1200 °C and 240 °C, respectively. The cooling behavior of the filaments controlled by the processing speed, is crucial to determine the fiber diameter and in turn the constructive design of the filament haul-off, as well as the commingling and the winding process. Besides the circular cross sections of GF with diameters, D_f , of 12–24 μm , the PP filament diameter, D_m , is varied in the region of 12–45 μm according to processing conditions.

The unidirectional fiber-reinforced polymer composites made of commingled yarns were processed in PC controlled long-term cycle (heating, consolidation, and cooling

in the mould) at a temperature of 225 °C for 45 min. In detail, heating from ambient temperature to 225 °C took 23 min at a pressure of 0.5 MPa, followed by hot pressing at 3 MPa for 2 min and cooling down to 40 °C for 20 min was applied. During cooling the pressure was kept constant at 3 MPa. To investigate the interfacial adhesion between the GF fiber and PP matrix, micro composites were prepared for the single fiber pull-out test. The single fiber was accurately embedded in the matrix (Borealis HD 120M with 2% Exxelor P1020) with embedding lengths of 800 μm .

Characterization

The distribution homogeneity of reinforcement and matrix components of the hybrid yarns were analyzed by an optical microscope (OM) using polished cross sections of yarns/composites embedded in epoxy. Atomic force microscopy (AFM, Digital Instruments D3100, USA) is used to determine the changes of the surfaces roughness of GF and PP fibers due to the different surface modification [20]. The topography of samples was studied in tapping mode. During the scanning in the tapping mode AFM, phase shifts, i.e., changes in the phase angle of vibration with respect to the phase angle of the freely oscillating cantilever, recorded simultaneously with height changes, are present as a phase image. The phase images reveal differences in surface properties of the material which are currently only qualitative in nature, which were produced using the following settings: a setpoint voltage equal to 50–55% of the free vibrational amplitude within a range from 2.0 V to 2.5 V and integral and proportional gains of 0.2 and 2.0, respectively. The difference between the setpoint and the free amplitude is directly related to the amount of force applied to the surface during imaging.

The influence of the hot pressing conditions on the molecular weight and the molecular weight distribution was studied using the high temperature gel permeation chromatography (HT-GPC). The number average molecular weight M_n and the weight average molecular weight M_w , were obtained and the ratio M_w/M_n was used to determine the width of the molecular weight distribution for PP in composites. 1,2,4 Trichlorobenzene was used to solve the samples at a temperature of 150 °C. As analysis tool a PL-GPC220 (Polymer Lab.) was used equipped with two PL-MIXED-B-LS Columns. The DSC measurements were performed using a DSC7 (Perkin Elmer, USA) equipped with the Pyris-software in a temperature range from –60 °C to 210 °C. The temperature and heat of transition were calibrated with In and Pb standards. The heating rate used was always 20 K/min and the molten state was kept for 2 min every times at 210 °C to destroy



Fig. 1 Pilot plant equipment for online commingled yarn spinning of GF and PP. The insert shows the intermingling of glass filaments (perpendicular) and polypropylene filaments (from right hand side)

the thermal history and in that way the pre-existing crystalline nuclei.

Mechanical testing

The tensile strength of single GF fiber was measured using the Fafegraph mechanical testing device (Fa. Textechno) equipped with a 100 cN force cell. The gauge length is 20 mm and the cross velocity is 10 mm/min under 65% relative humidity and 20 °C according to specification EN ISO 5079. Based on a vibration approach, the diameter of each selected fiber, D_f , was calculated from the fineness value which was determined by using a Vibromat ME (Fa. Textechno) according to specification EN ISO 53812 and ASTM D 1577. To verify the effect of surface properties on the statistical distribution of fiber tensile strength, the failure probabilities were fitted through the least squares method by single two-parameter Weibull model [25] using

$$P = 1 - \exp \left[- \left(\frac{\sigma}{s_0} \right)^{m_0} \right] \tag{1}$$

where P is the cumulative probability of failure ($i/(n + 1)$) at the tensile stress σ . The parameters m_0 and s_0 are the Weibull modulus and the scale factor of fractured fibers, respectively.

The single fiber pull-out test was carried out on a self-made pull-out apparatus with force accuracy of 1 mN and

displacement accuracy of 0.07 μm with identical pull-out velocities (0.01 $\mu\text{m/s}$) at ambient temperature. From each force–displacement curve, the force at start of debonding, F_d , the maximum force F_{max} , and the embedded length l_e were determined. The fiber diameter D_f of each pulled-out fiber was measured with an optical microscope. Each GF/PP combination was evaluated by about 15 single tests. The apparent adhesion strength τ and the critical inter-phase energy release rate, G_{ic} were calculated, according to

$$\tau = F_{max} / \pi D_f l_e \tag{2}$$

$$F_d = \pi (D_f / 2)^2 \left(-p + \sqrt{p^2 - q(G_{ic})} \right) \tag{3}$$

where p and $q(G_{ic})$ are terms depending on fiber and matrix mechanical properties and specimen geometry; their expressions and the derivation are given in [26], based on the theory originally presented in [27].

The transverse tensile strength σ_t is measured according to specification ISO 527 with a velocity of 1 mm/min, whereas cap strips are applied on the ends of the specimens ($2 \times 10 \times 140$ mm). The intralaminar shear strength τ_c of samples ($10 \times 10 \times 4$ mm) is measured by a self-made compression shear test equipment with a deformation velocity of 1 mm/min.

Fig. 2 Optical microscopy images of polished cross sections of GF/PP composites made by (a) online commingled and (b) air textured yarns

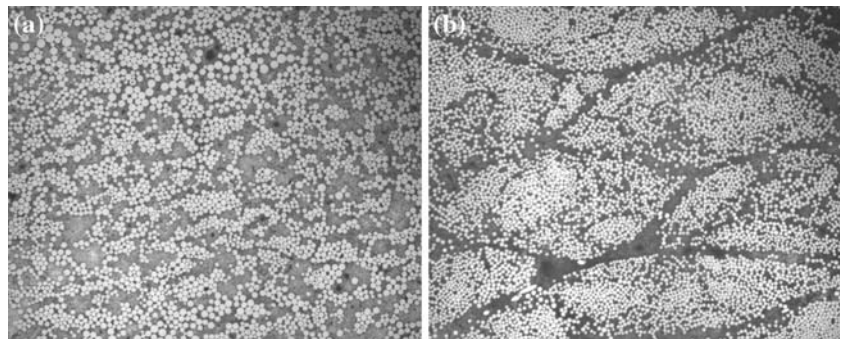
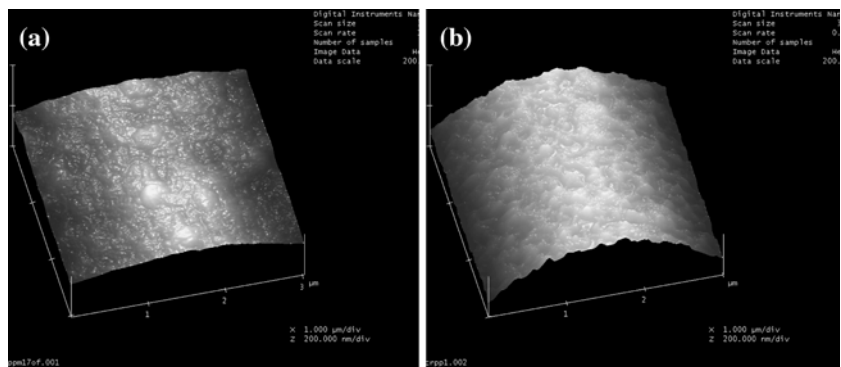


Fig. 3 AFM topography images of (a) PP filament without finish, (b) GF filament with sizing G consisting of aminosilane and maleic anhydride grafted nano-dispersed PP film former designed for high adhesion strength ($x, y = 3 \mu\text{m}$, $z = 400$ nm)



Results

Impregnation homogeneity influenced by texturing process and the properties of the hybrid yarns

We first examined the distribution homogeneity of reinforcement and matrix components in the hybrid yarns. A qualitative description is by the flow distance of either polymer or fibers, that is to say, the smaller the resin-rich area and the larger the average distance between fibers, the better is the impregnation homogeneity of the fibers with matrix. The different texturing process arrangements in hybrid yarns have remarkable effects on the distribution of fiber in matrix after hot compression processing as shown

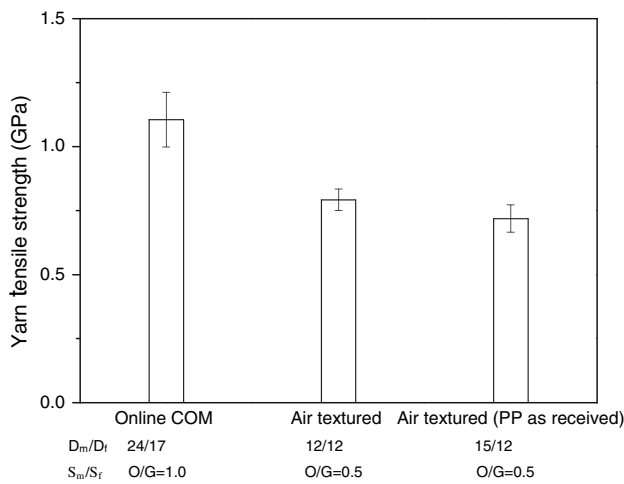


Fig. 4 Comparison of yarn tensile strengths of online commingled and air textured yarns with diameters of matrix and reinforcement filaments (D_m/D_f , μm) and surface modification (S_m/S_f , wt%) (G glass sizing, O no finish). Error bars represent standard deviations

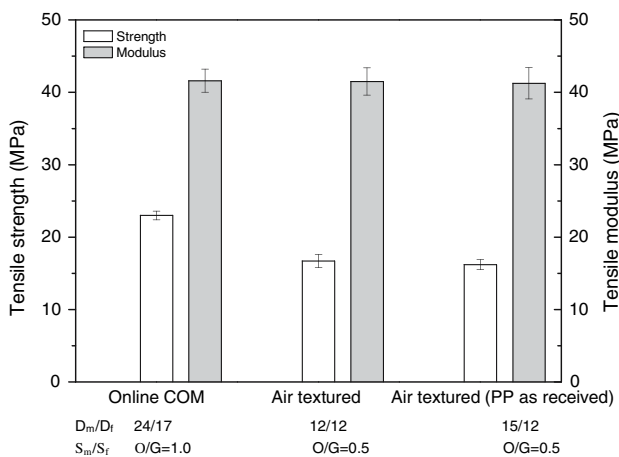


Fig. 5 Comparison of transverse tensile strengths and Young’s moduli of unidirectional composites (fiber volume fraction of 50 %) made out of online commingled and air textured yarns. Error bars represent standard deviations

in Fig. 2. It can be seen from the polished cross sections of the composites that homogeneous distribution patterns of GF surrounded by PP matrix for online commingled yarns is better than that of air-textured yarns. There was no significant difference found in the distribution homogeneity for different samples with the optimised sizings and finishes used for either the matrix and reinforcement filaments. This suggests that fiber surface properties do not affect the distribution homogeneity during texturing process and in turn the compression moulding where the

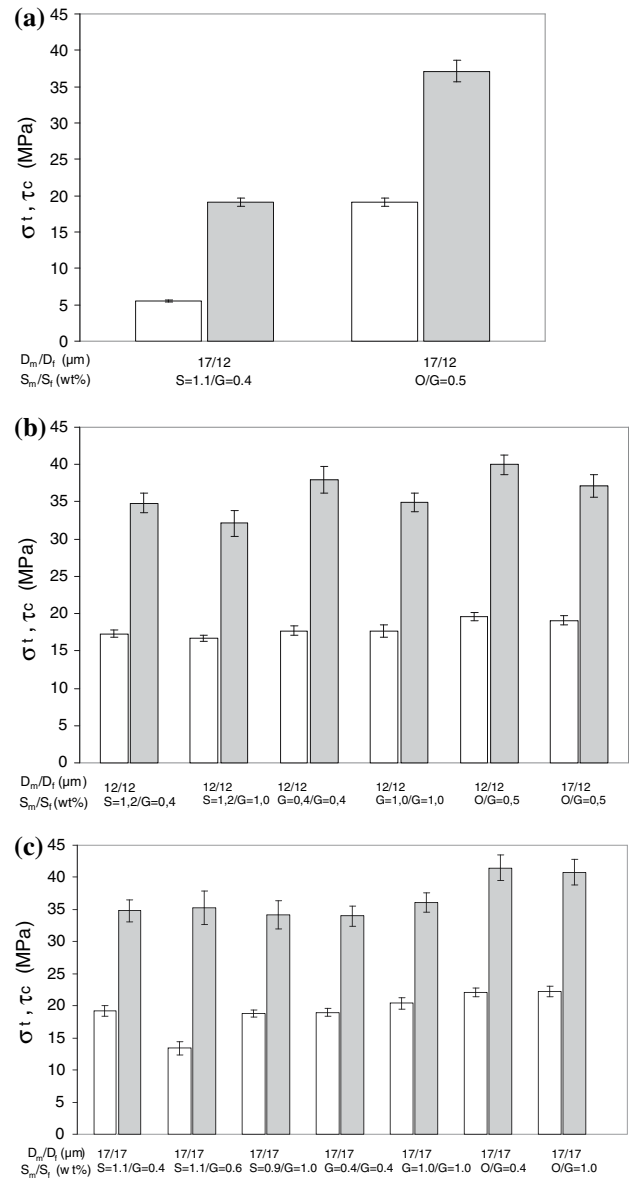


Fig. 6 Comparison of transverse tensile strength (white) and intralaminar shear strength (grey) of unidirectional composites with fiber volume fraction of 50% with varied (a) PP polymers (b) and (c) diameters of matrix and reinforcement filaments (D_m/D_f) and surface modification (S_m/S_f) of commingled yarns (S standard finish, G glass sizing, O no finish). Error bars represent standard deviations

Table 1 Summary of obtained values for M_n , M_w , and M_w/M_n for PP-granules and PPM-fiber as raw material and after hot pressing varied by filament diameter and sizing/finish compared to commercial Twintex-fiber

Sample	M_n [g/mol]	M_w [g/mol]	M_w/M_n
PP-granules	116,400	195,500	1.68
PPM-fiber	138,000	215,900	1.56
D_m/D_f (μm): 12/12, S_m/S_f (wt%): $S = 1.2/G = 0.4$	102,400	170,200	1.66
D_m/D_f (μm): 17/17, S_m/S_f (wt%): $G = 0.4/G = 0.4$	92,800	168,200	1.81
D_m/D_f (μm): 17/17, S_m/S_f (wt%): $0/G = 0.4$	97,100	170,100	1.75
D_m/D_f (μm): 17/12, S_m/S_f (wt%): $S = 1.2/G = 0.4$	96,200	161,900	1.68
D_m/D_f (μm): 24/12, S_m/S_f (wt%): $0/G = 0.4$	105,600	179,100	1.70
Twintex-fiber	88,400	166,600	1.88

fiber movement is negligible for the continuous yarns. AFM topography images of GF and PP filaments show equal values of the average and maximum height surface roughness of 4–6 nm or 40–60 nm, respectively. The sizing G applied to GF as described in Section “Materials” containing nano-dispersed grafted PP film former but no carbon nanotubes was designed to reach the same surface roughness as for PP without finish (Fig. 3). For systems with the variation of filament diameters in range of $D_f = 12$ – $17 \mu\text{m}$, $D_m = 12$ – $24 \mu\text{m}$, we also do not detect remarkable differences in the distribution homogeneity of the two components. A further increase of the diameters of GF and PP to average values of 24 and 45, however, a homogeneous arrangement of the two components is impeded.

Yarn and composite properties of online commingling and air texturing compared

Figure 4 displays the yarn tensile strengths of online COM and two different air textured COM yarns. The online COM and air textured hybrid yarns compared contain the same sizing G , but no finish on the PP-filaments. Furthermore, the PP-matrix and modification is kept constant. The ratios D_m/D_f are 24/17 for online COM and 12/12 for air textured yarns, respectively. The fiber volume content is kept constant at 50%. In comparison, the commercial PP-filaments used are unknown in both polymer and finish. Clearly, the air textured yarns show a significant decay of the tensile strength, which is due to damage of glass filaments caused by the high air pressure during intermingling. The two air textured yarns show a variation of the tensile strength which might be due to the different strand integrity introduced by sizings/finishes. Similarly, we observed a remarkable improvement in mechanical properties of the composites made by the online hybrid yarns (Fig. 5), although the diameters of the filaments are greater than those of the air-textured yarns. Particularly in transverse tensile strength a 30% increase was achieved, which is attributed to better impregnation homogeneity and different interfacial states, as being introduced by the unknown commercial PP and finish on it. The air textured yarns

possess somewhat reduced Young’s modulus values induced by disorientations of reinforcement filaments.

Composite properties in dependence of the polymer/surface modification and the ratios of fiber diameters

We then investigated in detail the mechanical properties of unidirectional composite plates made of commingled yarns

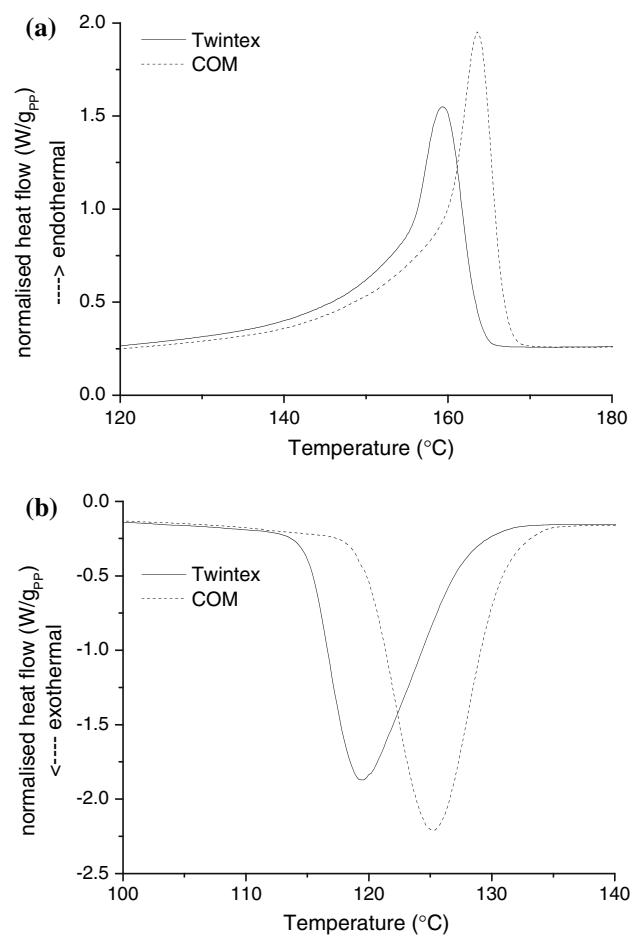
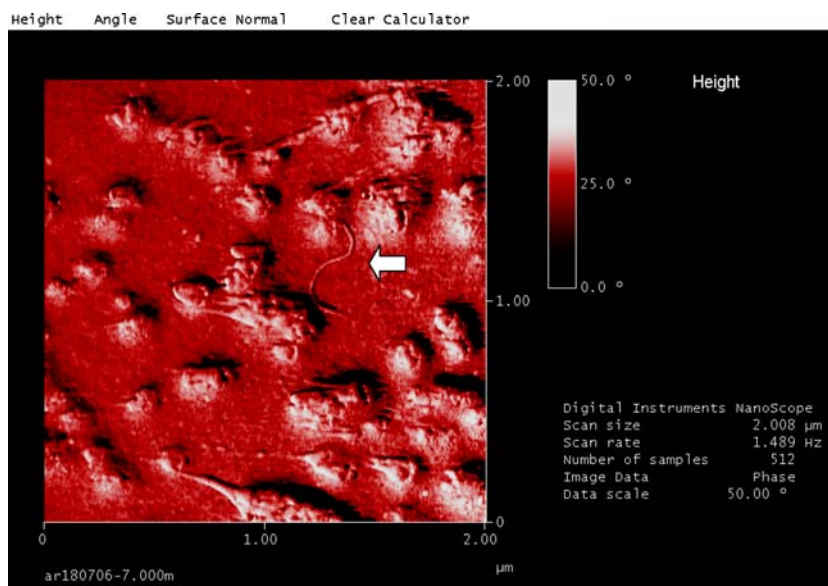


Fig. 7 Comparison of (a) melting and (b) crystallization behavior of online commingled yarns investigated in this work (COM means in detail the combination of D_m/D_f : 12/12, S_m/S_f : $S = 1.2/G = 0.4$) and Twintex

Fig. 8 AFM phase image of a sized glass fiber surface. The arrow shows a SWNT within the sizing



(Fig. 6). It shows that the use of modified PP leads to significantly increased transverse tensile strengths and intralaminar shear strengths compared to homo-PP (Fig. 6a). In comparison with unfinished PP-filaments the standard finish used for homo-PP filaments deteriorates the transverse tensile strength only marginally (cf. Fig. 6b). However, the huge difference is due to the presence and absence of covalent bonds for PPM and homo-PP, respectively.

It is well known that unidirectional fiber reinforced composites have a very low transverse tensile strength. This strength is normally lower than the strength of the pure matrix and limits the performance of the composite system. Assuming a perfect interfacial adhesion in the

laminates, the transverse tensile strength, σ_t , can be estimated from [28]

$$\sigma_t = \left[1 - (\sqrt{V_f} - V_f) \left(1 - \frac{E_f V_m + E_m V_f}{E_f} \right) \right] \sigma_m \quad (4)$$

where σ_m is the matrix tensile strength. V and E are volume fraction and Young's modulus of the materials and the subscripts f and m refer to the properties of the fiber and the matrix, respectively. Taking $E_f = 72$ GPa, $E_m = 1.2$ GPa, $\sigma_m = 30$ MPa for E-glass fiber and PP, respectively, we can calculate σ_t to be ≈ 26.9 MPa, which is a fairly good agreement with experimentally determined values of the composites with the modified PP matrix, while it is much higher than that of the composites with the homo-PP associated with poor interfacial adhesion. This indicates a predominant effect of the interface adhesion properties on transverse tensile properties of laminated composites. It is evidenced that the enhancement of the adhesion by acid–base interactions or covalent bonds is possible only by the functionalization of the PP combined with effective sizing on GF.

The additional application of spin finishes (standard finish or glass sizing, respectively) on the matrix filaments does not improve the mechanical properties of the composites, whereas the composites with un-finished PP filaments (O) show marginal higher transverse tensile strengths and compression shear stresses (Fig. 6b, c). This is not surprising since the additional finishes might result in excessive sizing molecules, i.e. physisorbed layers which reduce fiber/interphase adhesion. The variation of the filament diameters and sizing concentration cause neither a more homogeneous distribution nor improved composite properties within the variation range.

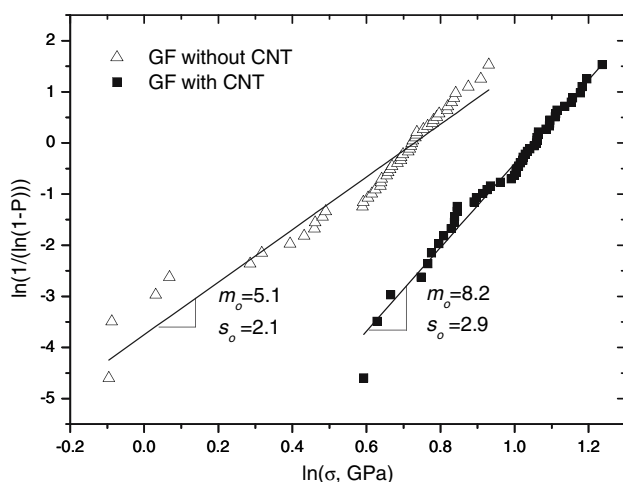
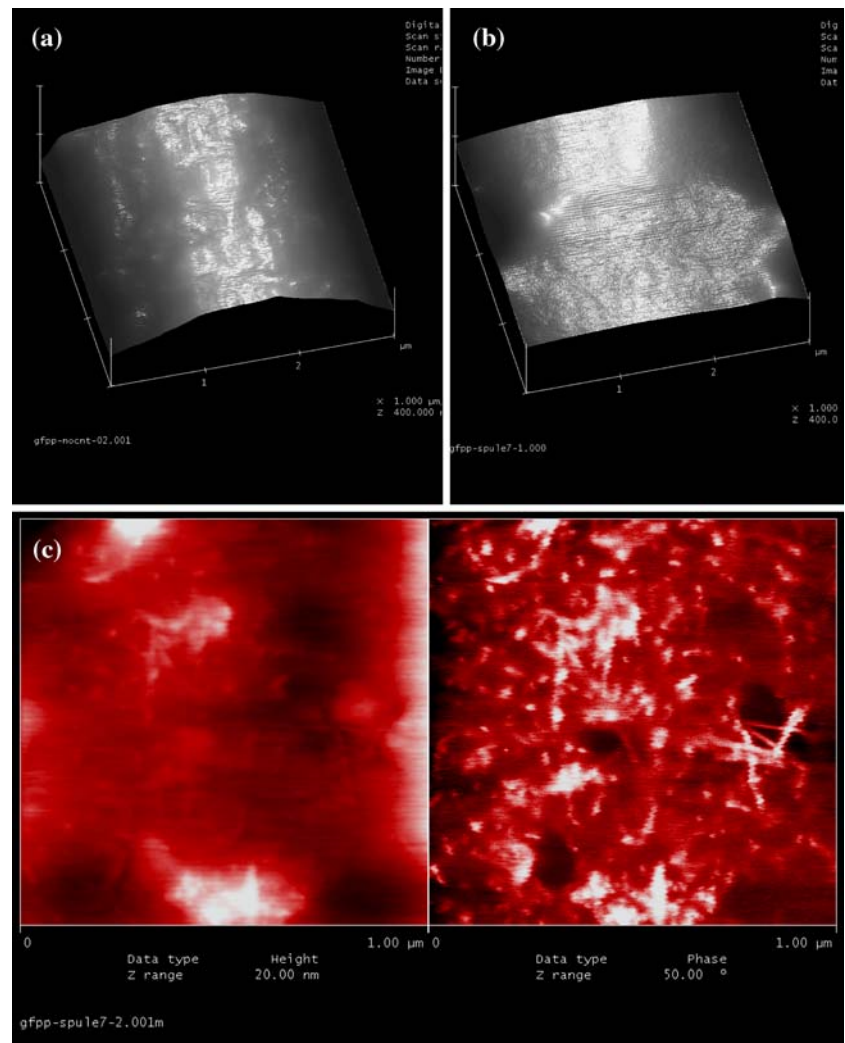


Fig. 9 Weibull plots of fiber fracture probability for GF with/without SWNTs in the sizing

Fig. 10 AFM topography images of fracture surfaces of (a) GF without SWNTs and (b) GF with SWNTs in sizing after fiber pull-out test ($x, y = 3 \mu\text{m}$, $z = 400 \text{ nm}$). (c) AFM topography and phase images of GF with SWNTs in sizing ($x, y = 1 \mu\text{m}$, $z = 20 \text{ nm}$, 50°)



Polymer properties influenced during processing

The changes of the molecular weight (granules, polymer filaments, consolidated composites) have been determined using HT-GPC. The molecular weights of the differently consolidated specimens, according to Table 1, are comparable within the variation range of the method (10%). Furthermore, the average molecular weight of the granules is about 20% greater than that of the consolidated PP. It should be noted that for spinning trials non-stabilised PP was used and the hot pressing of composite plates was carried out in a long-term cycle (heating, consolidation, and cooling in the mould) at a temperature of 225°C for about 45 min. The increase of the molecular weight from the granules to the fibers is due to the PP functionalization with 2 wt% Exxelor P1020. The enhancement can be explained by the maleic anhydride grafts initiating the formation of branched chains, which interact with other polymer chains [29]. It is interesting to note that both the melting peak temperature and onset crystallization

temperature of the online COM show higher values compared to commercial Twintex-fiber (see Fig. 7). These higher transition temperatures suggest that the crystals formed within the COM are of higher quality, that is to say, the spherulites of a high order of alignment and compact packing, as a higher quality crystal generally has a higher melting temperature. The higher onset crystallization temperature of the online COM implies an opportunity to decrease the cycle time.

Nano-structured surfaces of online commingled yarns and model single fiber composites

Compared with other work distributing at least 0.3 wt% carbon nanotubes homogeneously over the whole polymer matrix [30], we concentrated SWNTs or differently functionalized MWNTs in the interface by applying surface sizings with 0.04 wt% SWNTs related to the sizing or 6.7×10^{-4} wt% related to the PPM-matrix of the composite. In detail, we present results for the sizing G applied

to glass fibers and PPM-filaments, as described in Section “Materials” and Fig. 6c (D_m/D_f (μm): 17/17, S_m/S_f (wt%): 0/G = 1.0), and added 0.04 wt% SWNTs related to the sizing. During online commingling the nano-structured surfaces are made simultaneously on GF and PP filaments. In the nano-dispersed sizing we could reveal SWNTs in AFM phase images of GF (cf. Fig. 8). Although the concentration of CNT is very small, an effect of increased glass fiber tensile strength could be revealed. Interestingly, the average strain of the GF with SWNTs increased by 10%. As shown in Fig. 9, both the Weibull plot lines and Weibull modulus, m_o , of nanotube coated systems shift to higher values corresponding to healing of surface flaws, which implies that the strength-controlling surface defects have lower heterogeneity of distribution and the size of defects is reduced [22]. In other words, the healed flaws on the fibers with SWNTs show similar flaw size, severity and homogeneity relative to those without SWNTs.

The interfacial parameters in GF/PP systems were characterized by single fiber pull-out tests. The data indicates a local adhesion strength of 30.2 MPa with SWNTs compared with 22.1 MPa for the same GF/PP/sizing system without SWNTs. The critical interface energy release rates determined are 31.8 and 14.0 J/m², correspondingly. The significant improvement of adhesion strength seems to be caused by a different failure mechanism (local interfacial bonding and crack bridging). Due to the mechanical interlinking with SWNTs the roughness of the fracture surfaces is increased (Fig. 10a, b) and the phase image (Fig. 10c) shows material inhomogeneity possibly caused by carbon nanotubes. Overall, the in-situ commingling process technology and nanostructuring coatings show promising potential in cost-effective processing continuous fiber thermoplastic composites for different applications.

Conclusions

The commingling technique opens many opportunities to modify hybrid yarns and composites using different ratios of filaments, filament diameters, finishes, and polymer properties. The online commingling is a universal basis for tailoring new composites by both PP functionalised with maleic anhydride grafted PP and by designed interfaces to achieve improved adhesion strength and enhanced composites properties. The concentration of smallest amounts of SWNTs in the interface can be utilised to introduce multifunctional effects such as improved mechanical properties, modified morphology of interphases, and new fracture mechanisms. Other polymers and polymer filament geometries are foreseen to study the influences on both commingling and composites homogeneity.

Acknowledgments This work was supported by the German Research Foundation (DFG) within the Collaborative Research Centre ‘Textile-reinforced composite components for function-integrating multi-material design in complex lightweight applications (SFB639)’. The authors are indebted to Dr. H. Brüning, B. Tändler and N. Smolka (Spinning of PP), W. Ehrentraut, F. Eberth, R. Plonka (Spinning of GF) and Jianwen Liu for technical assistance.

References

1. Svensson N, Shishoo R (1998) J Thermoplastic Compos Mater 11:22
2. Ruan XP, Chou TW (1996) Comp Sci Technol 56:198
3. http://www.tu-dresden.de/mw/ilk/sfb639/sfb_en.html
4. Wakeman MD, Cain TA, Rudd CD (1998) Comp Sci Technol 58:1879
5. Alagirusamy R (2004) J Ind Textiles 33:223
6. Hamada H, Maekawa Z, Ikegawa N, Matsuo T (1993) Polym Compos 14:308
7. Ye L, Friedrich K (1993) Comp Sci Technol 46:187
8. Ye L, Friedrich K (1993) J Mater Sci 28:773 DOI: 10.1007/BF01151255
9. Mäder E, Bunzel U, Schemme M (1994) Chemiefasern/Textilindustrie 37:11
10. Offermann P, Wulfhorst B, Mäder E (1995) Technische Textilien/Technical Textiles 38:55
11. Shonaika GO, Hamada H, Maekawa Z (1996) J Thermoplastic Compos Mater 9:76
12. Stumpf H, Mäder E, Baeten S, Pisanikovski T, Zäh W, Eng K, Andersson CH, Verpoest I, Schulte K (1998) Composites/Part A 29:1511
13. Mäder E, Skop-Cardarella K (1997) Key Eng Mater 137:24
14. Bogoeva-Gaceva G, Mäder E, Queck H (2000) J Thermoplastic Compos Mater 13:363
15. Long AC, Wilks CE, Rudd CD (2001) Comp Sci Technol 61:1591
16. Vendramini J, Bas C, Merle G (2000) Polym Compos 21:724
17. Bernet N, Michaud V, Bourban PE, Manson JAE (2001) Composites Part A 32:1613
18. Putnoki I, Moos E, Karger-Kocsis J (1999) Plastics, Rubber Compos 28:40
19. Lariviere D, Krawczak P, Tiberi C, Lucas P (2005) Polym Polym Compos 13:27
20. Gao SL, Mäder E (2002) Composites/Part A 33:559
21. Tong L, Mouritz AP, Bannister M (2002) 3D fibre reinforced polymer composites. Elsevier Science, Oxford
22. Gao SL, Mäder E, Plonka R (2007) Acta Mater 55:1043
23. Report Aif-Nr. 322d (1993) Report Aif-Nr. 10039 B (1996) Report Aif-Nr. 11644b (2000) Leibniz-Institut Für Polymerforschung Dresden e.V
24. Online.Hybridgarnspinnen Von Glasfaser- Und Thermoplastfilamenten (2005) Jahresbericht Leibniz-Institut Für Polymerforschung Dresden e.V., p 64
25. Weibull W (1951) J Appl Mech 18:293
26. Zhandarov S, Pisanova E, Mäder E (2000) Compos Interface 7:149
27. Nairn JA (2000) Adv Compos Lett 9:373
28. Kaw AK (2006) Mechanics of composite materials, 2nd edn. ISBN: 0-8493-1343-0, Crc Press
29. Mäder E, Rothe C, Liu JW (2005) Proc Technomer. Chemnitz, p 39 (CD-ROM: 1–15)
30. Gojny FH, Wichmann MHG, Fiedler B et al (2005) Comp Sci Technol 65:2300